Technical Report
RAL-TR-95-034

A Guide to Critical Scattering Measurements using Time of Flight Neutron Diffraction

M Hagen and S J Payne

August 1995

COUNCIL FOR THE CENTRAL LABORATORY OF THE RESEARCH COUNCILS

Enquiries about copyright, reproduction and requests for additional copies of this report should be addressed to:

The Central Laboratory for the Research Councils
Library and Information Services
Rutherford Appleton Laboratory
Chilton
Didcot
Oxfordshire
OX11 0QX
Tel: 01235 445384 Fax: 01235 446403
E-mail library@rl.ac.uk

ISSN 1358-6254

A GUIDE TO CRITICAL SCATTERING MEASUREMENTS USING TIME OF FLIGHT NEUTRON DIFFRACTION

M. Hagen and S. J. Payne

Department of Physics, Keele University, Staffordshire, ST5 5BG, U.K.

and

ISIS Facility, Rutherford Appleton Laboratory, Chilton

Didcot, Oxfordshire OX11 0QX

Abstract

A description is given of how the time of flight neutron diffraction technique can be used to measure critical scattering at magnetic or structural phase transitions. This includes discussions of sample mounting requirements, actual scan geometries and data analysis methods. Also included are warnings about problems such as primary extinction and multiple scattering which can effect this type of experiment.

Contents

1 Introduction

1.1 The Guide

This guide outlines the background knowledge that is required to carry out a time of flight critical scattering measurement. It cannot, of course, cover all possible experiments that can be conceived but we hope it will prove useful to people in flagging many of the things that need to be thought about for such an experiment. We don't intend to review in detail the current theory of critical phenomena or for that matter the relationship between neutron scattering and critical phenomena. The reader who would like more background information on these subjects might like to refer to the texts by Yeomans [1], Collins [2] and Cowley [3]. Instead we will concentrate on the practicalities of performing a critical scattering measurement by the time of flight technique.

The rest of this first section of the guide gives a brief overview of the features in critical phenomena that can be obtained by neutron scattering techniques. Section 2 sets out the notation and theory for time of flight diffraction from single crystal samples. Section 3 highlights areas that need to be considered when planning an experiment. The performance of the experiment itself is discussed in sections 4 (Bragg peak intensity measurements) and 5 (critical scattering). Finally section 6 contains a brief summary.

1.2 Critical Phenomena, Phase Transitions and Order

The term critical phenomena refers to the behaviour of systems close to a phase transition from one state to another. Quite often these two states are an ordered and a dis-ordered

state (eg. an anti-ferromagnetic and a paramagnetic state). If the transition is a continuous one then the driving force behind the transition is the growth of short range order (fluctuating microregions) as the transition is approached [1]. The average size of these short lived fluctuating microregions is known as the *correlation length*, ξ, and it is these regions which give rise to the *critical scattering* which can be observed around the transition temperature [2]. By measuring this critical scattering with neutrons it is possible to extract values for the correlation length and susceptibility as a function of temperature [3].

The intrinsic lineshape $S(\mathbf{q})$ of the critical scattering is often a Lorentzian or Lorentzian squared form such as ;

$$S(\mathbf{q}) = \chi L(\mathbf{q}) + \chi' \left[L(\mathbf{q})\right]^2 \tag{1}$$

where

$$L(\mathbf{q}) = \frac{1}{1 + \left(\frac{q_L - q_L^0}{\kappa_L}\right)^2 + \left(\frac{q_T - q_T^0}{\kappa_T}\right)^2 + \left(\frac{q_V}{\kappa_V}\right)^2} \tag{2}$$

and the experimentally measured intensity is the convolution of this critical scattering lineshape with the instrumental resolution function. If a non-linear least squares fitting method is used to fit the measured intensity (see section(5.6)) then the HWHM values of the critical scattering lineshape(s) can be extracted. These HWHM values, which are usually refered to by the symbol κ (with appropriate subscripts if necessary), are known as the inverse correlation length(s) and are related to the correlation length(s) by the equation $\kappa = 2\pi/\xi$. The temperature dependence of κ is described by a power law form given by ;

$$\kappa = \kappa_0 t^{\nu} \tag{3}$$

where ν is the *critical exponent*, κ_0 is the *critical amplitude* and t is the reduced temperature given by $t = |T - T_c|/T_c$, where T_c is the critical temperature and T is the temperature of the sample.

In addition to the κ values, the amplitude of the critical scattering can also be obtained from the lineshape fitting. The amplitude is related to the susceptibility χ of the material which can also be described by a power law given by

$$\chi = \chi_0 t^{-\gamma} \tag{4}$$

where γ is the critical exponent and χ_0 is the critical amplitude.

Apart from studying the behaviour of the critical scattering with neutrons it is also possible to study the behaviour of structural or magnetic Bragg peaks below the critical temperature. If the relevant Bragg peak occurs because of the long range order below the transition temperature then it is usually related to the square of the *order parameter* for that phase. Consequently it also follows a simple power law of the form

$$I = I_0 t^{2\beta} \tag{5}$$

where β is the critical exponent and I is the intensity of the Bragg peak.

There are other external parameters, apart from temperature, that can be altered to cause a phase transition. In a magnetic material, for example, a transition can occur when an external magnetic field is applied to an antiferromagnet. If the field is large enough it is possible to reverse the orientation of the magnetic moments antiparallel to the field, thereby destroying the long range antiferromagnetic order and creating long range ferromagnetic order. In ferroelectric materials a phase transition can be induced by

the application of an electric field to polarise the material. These are just a few of the many possible phase transitions that can be investigated. It is also the case that transitions do not have to happen in a continuous manner, ie. transitions can be discontinuous. In this case instead of falling steadily to zero, the magnetisation in a ferromagnet could change precipitously from a non-zero value to zero. In all of these cases neutron scattering can play an important role by measuring the size of the correlations and the value of the order parameter as a function of temperature.

2 Time of Flight Techniques

2.1 Introduction

In the following sections we describe how time of flight techniques can be employed to carry out neutron diffraction measurements from single crystal samples. The formalism which we use to describe this process is different to that used by crystallographers when discussing single crystal diffraction and is much more closely related to inelastic neutron scattering. This is because critical scattering measurements have tended in the past to be carried out by people whose training has been in inelastic scattering. Since we ourselves have followed such a training we make no apology for sticking to this notation.

2.2 The Time of Flight Neutron Diffraction Technique for Single Crystals

At a spallation neutron source the neutrons are produced in pulses and the wavelengths /energies of the neutrons are determined by time of flight methods. For neutron diffraction it is usual to use a "white beam" technique where all of the wavelengths/energies in the incident pulse are allowed to scatter from the sample. Using this wavelength/energy dispersive technique it is possible to perform a radial scan in reciprocal space with a single detector. In the following two sections we describe how this technique can be used for measurements on single crystal samples. Initially we consider the case of just a single detector and then the use of a multi-detector.

2.2.1 A Single Detector Scan

The situation involving only one detector is as shown in figure(1). As the moderated neutrons travel towards the sample from the spallation source target the neutron pulse disperses because of the different neutron energies (and hence velocities) within the pulse. The incident neutrons with wavevectors k_i $(= 2\pi/\lambda)$ will be scattered from the sample at various angles. For example the neutrons scattered at an angle ϕ are recorded in the detector labelled D in figure(1) with a wavevector k_f. In the case of elastic scattering where no energy is transferred to the crystal then $k_i = k_f = k$ and k can be found through de Broglies relation for the momentum, $p = m_N v = \hbar k$. The velocity of the neutrons is given by $v = L/T$, where L is the distance from the moderator to the detector and T is the time taken for the neutrons to travel this distance. Therefore k is given by

$$k = \frac{m_N L}{\hbar T} \tag{6}$$

Hence by recording the neutrons entering the detector as a function of their flight time T, it is possible to calculate the wavevector k for each neutron detected.

The wavevector (momentum) transferred from the neutron to the sample in the scattering process is given by

$$\mathbf{Q} = \mathbf{k}_i - \mathbf{k}_f \tag{7}$$

This vector equation can be represented as a scattering triangle constructed in reciprocal space as shown in figure(2) where the magnitude of $\mathbf{Q}$ is given by:

$$Q = 2k \sin \frac{|\phi|}{2} \tag{8}$$

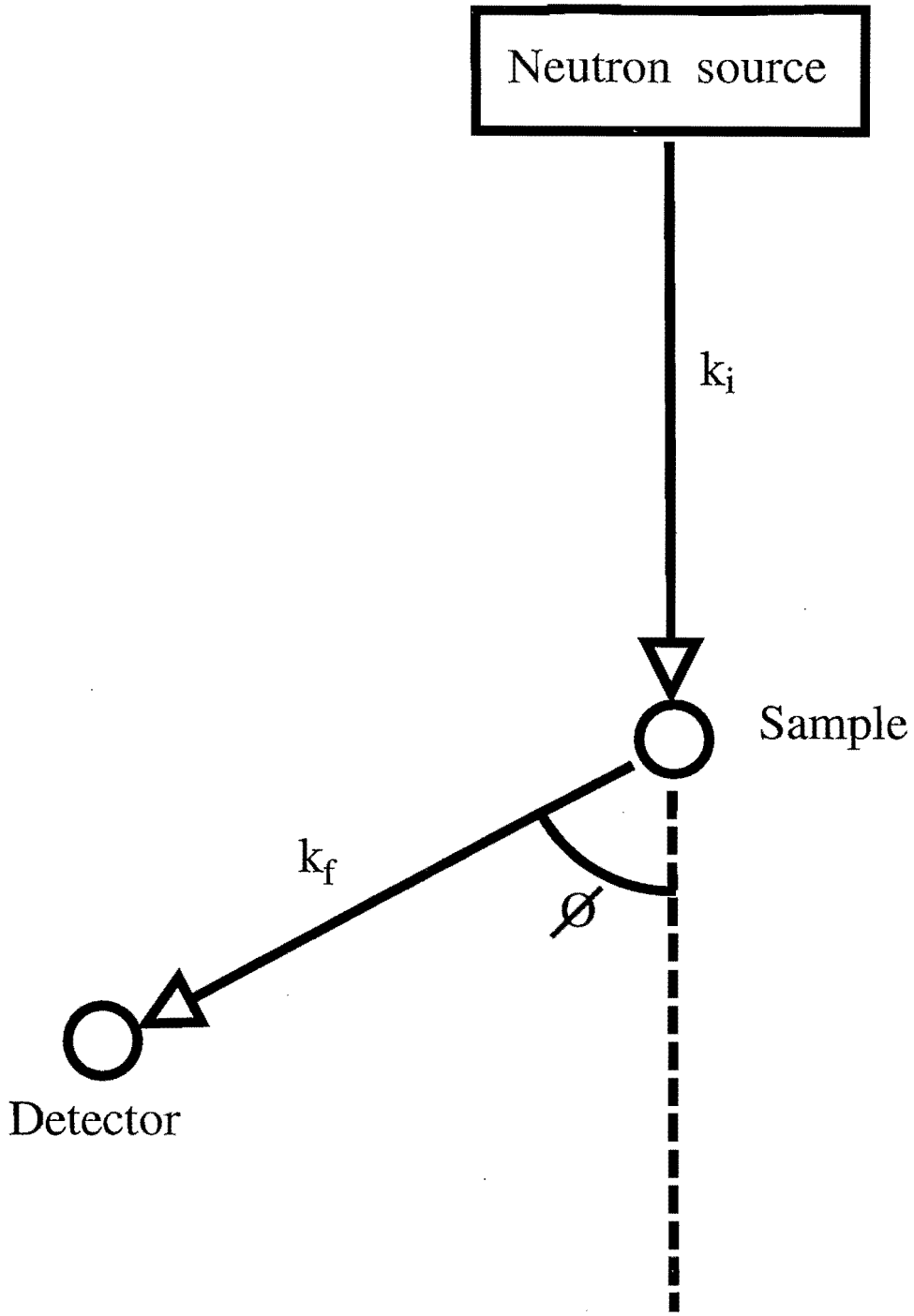

Figure 1: A schematic diagram is shown of the geometry used for single detector white beam neutron diffraction. The white beam pulse of neutrons travels down from the moderator to the sample where it is scattered. Those neutrons scattered at an angle ϕ to the incident beam are measured in the detector D

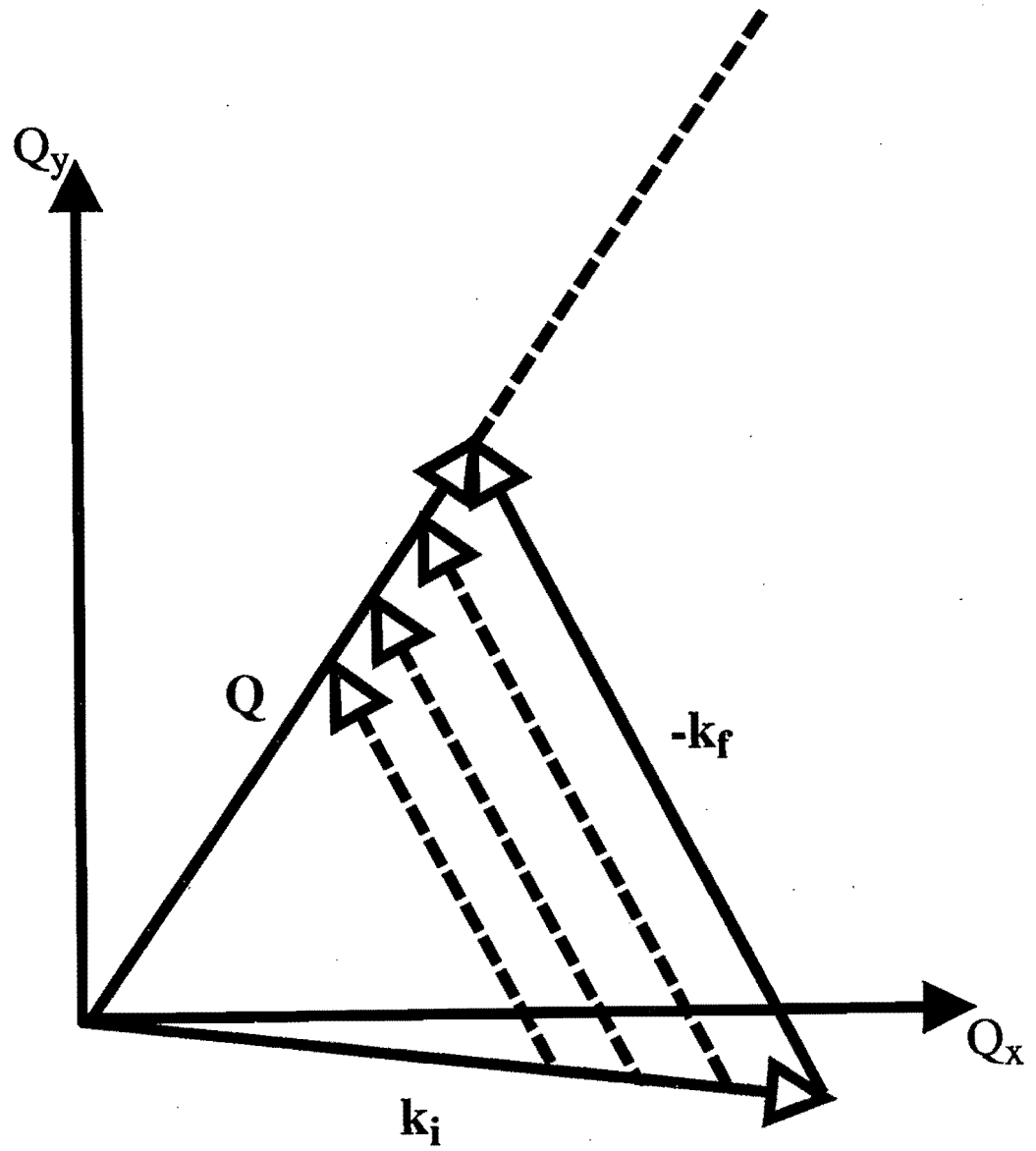

Figure 2: The path followed in reciprocal space by the scan performed by a single detector in the white beam neutron diffraction technique is shown. At each time step a vector triangle can be drawn following equations(6), (7) and (8).

Since ϕ is fixed for this detector Q varies with k according to equation(8) and k varies with T according to equation(6). Hence the length of Q is effectively scanned along a radial path in reciprocal space as a function of the flight time T.

The white beam time of flight technique using a single detector therefore performs a radial scan in reciprocal space for a single setting of the sample rotation angle ω and detector scattering angle ϕ. If the sample is rotated to an angle $\omega + \delta\omega$ and the detector left at angle ϕ then the new radial scan in reciprocal space is at an angle of $\delta\omega$ to the original. It is therefore possible to map out a region of reciprocal space by stepping the sample rotation angle (a rocking curve) and at each step performing a white beam time of flight scan. This type of measurement is often used to measure a Bragg peak where quite fine steps in ω are required. Alternatively if the sample rotation angle is kept fixed and the detector angle changed by $\delta\phi$ then the radial scan in reciprocal space is at an angle of $\delta\phi/2$ to the original. Although this type of scan, stepping ϕ, could also be used to map out a Bragg peak it has not been used in practice. If the ω and ϕ angles are varied in the ratio $\delta\omega : \delta\phi = 1 : 2$ then the direction of the radial scan in reciprocal space remains unchanged. However the neutron energy/wavelength at which a Bragg peak (or any other feature) on the radial scan is measured will change. This can be a useful scan to check if a Bragg peak (or any other feature) is sensitive to a particular neutron energy/wavelength (cf. section(5.5)).

2.2.2 Multi-Detector Scans

As discussed in the previous section the spectrum measured by a single detector in white beam time of flight diffraction is equivalent to a radial scan in reciprocal space. If however instead of using one detector a multi-detector (cf. figure(3)) is used then a "fan" of radial scans is measured in reciprocal space (cf. figure(4)).

On the PRISMA spectrometer at ISIS the multi-detector has a total of 16 available detectors. Clearly measuring 16 radial scans in parallel gives a much higher count rate than measuring a single radial scan. However it is not always the case that all 16 detectors can be used. There are a number of points which can restrict the number of "useful" detectors to fewer than 16, perhaps even just to 1.

If the angular separation of detectors is $\delta\phi$ then the separation of the radial "spokes" of the scans in reciprocal space is $\delta\phi/2$. In practice it is difficult to have $\delta\phi$ less than 1° in a multi-detector of helium tubes and so the separation of the spokes in reciprocal space is 1/2°. This is usually a much too coarse step to use for a Bragg peak rocking curve. In fact a Bragg peak rocking curve is usually done with a single detector as discussed in section(2.2.1). Although critical scattering is much broader in reciprocal space than a Bragg peak this may also still be too large a "rocking curve step". In this circumstance the sample rotation angle can be stepped to interleave the fans of radial spokes in reciprocal space to build up a grid of radial scans with suitably narrow angular steps between them in reciprocal space.

Another effect which can limit how many detectors can be effectively used comes about

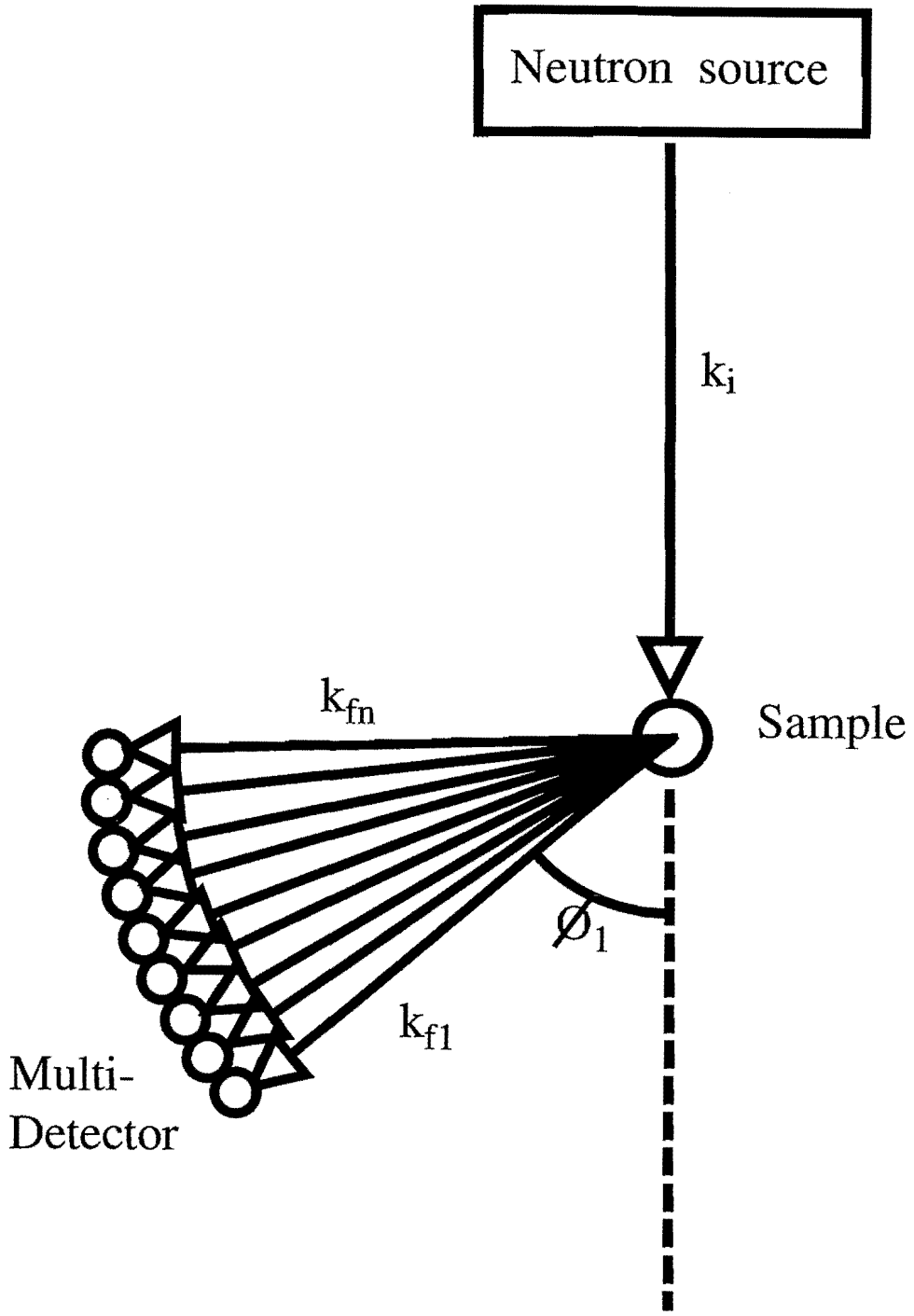

Figure 3: A schematic diagram is shown of the geometry used for multi-detector white beam neutron diffraction.

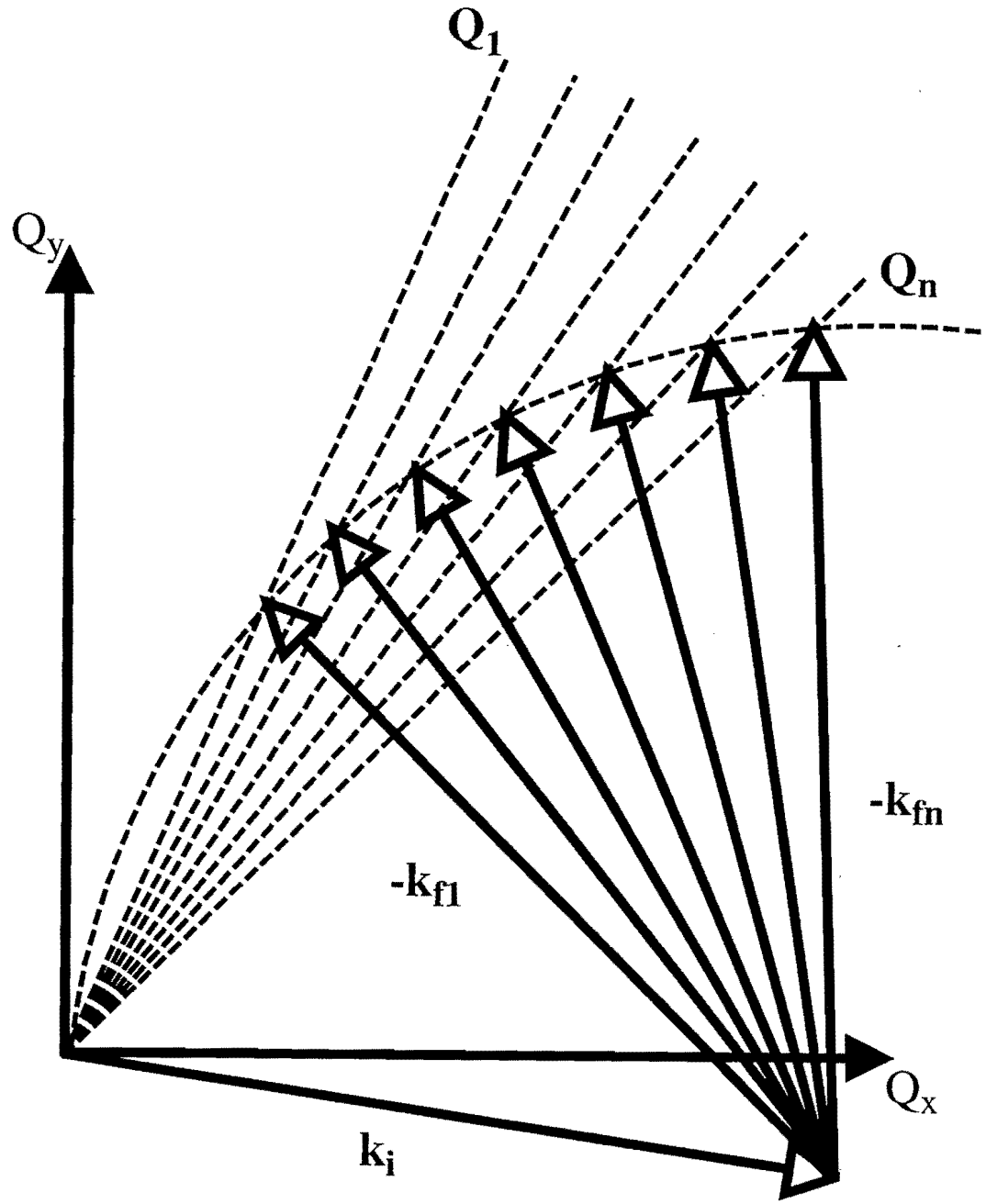

Figure 4: The fan of radial scans in reciprocal space generated by using a multi-detector in a white beam time of flight diffraction measurement is shown.

because the detectors are at slightly different ϕ angles. Consequently the same $|\mathbf{Q}|$ is measured in different detectors with different incident neutron energies. This means that the resolution and energy integration (see section(5.3)) conditions differ from detector to detector. Although such a variation will be accounted for in the data normalisation and analysis one generally doesn't want this variation to be too large. The range of such a variation, and how acceptable such a variation is, will depend upon the specific experimental circumstances but it is quite conceivable that as a consequence one may not wish to use all 16 detectors but only a fraction of them because of this.

Although it may not always be possible to take full advantage of all of the detectors in a multi-detector, the use of even only a fraction of them leads to a greatly increased count rate and the ability to quickly map out the contours of critical scattering at a particular temperature.

3 Experimental Preparation

3.1 Introduction

There are basically two things that need to be considered/done before starting a critical scattering experiment. The first is to mount the crystal ready for the experiment and the second is to consider what neutron energy to use for the experiment. Since good temperature control/stability is essential in a critical scattering experiment the sample mount/environment must take this into account. In section(3.2) we briefly describe our approach to this problem using a sample can. As a corollary to this, although it isn't a preparation, in section(3.3) we briefly describe how the samples temperature stability can be assessed. The choice of what neutron energy to use depends on many factors, some of which it is more appropriate to include in later sections rather than here. However one of the major factors in choosing the energy is that there should be a sufficiently good wavevector resolution to resolve the width of the critical scattering precisely enough. In section(3.4) we discuss how calculations of the resolution widths can be carried out.

3.2 Sample Preparation

Temperature stability is essential when performing critical scattering measurements and to help ensure this stability we have normally mounted the sample inside a purpose made aluminium sample can filled with helium exchange gas. A sketch of the can we have used is shown in figure(5). It is made solely from aluminium and comes in two parts, the body and the base. The circular base and the body have around their circumference

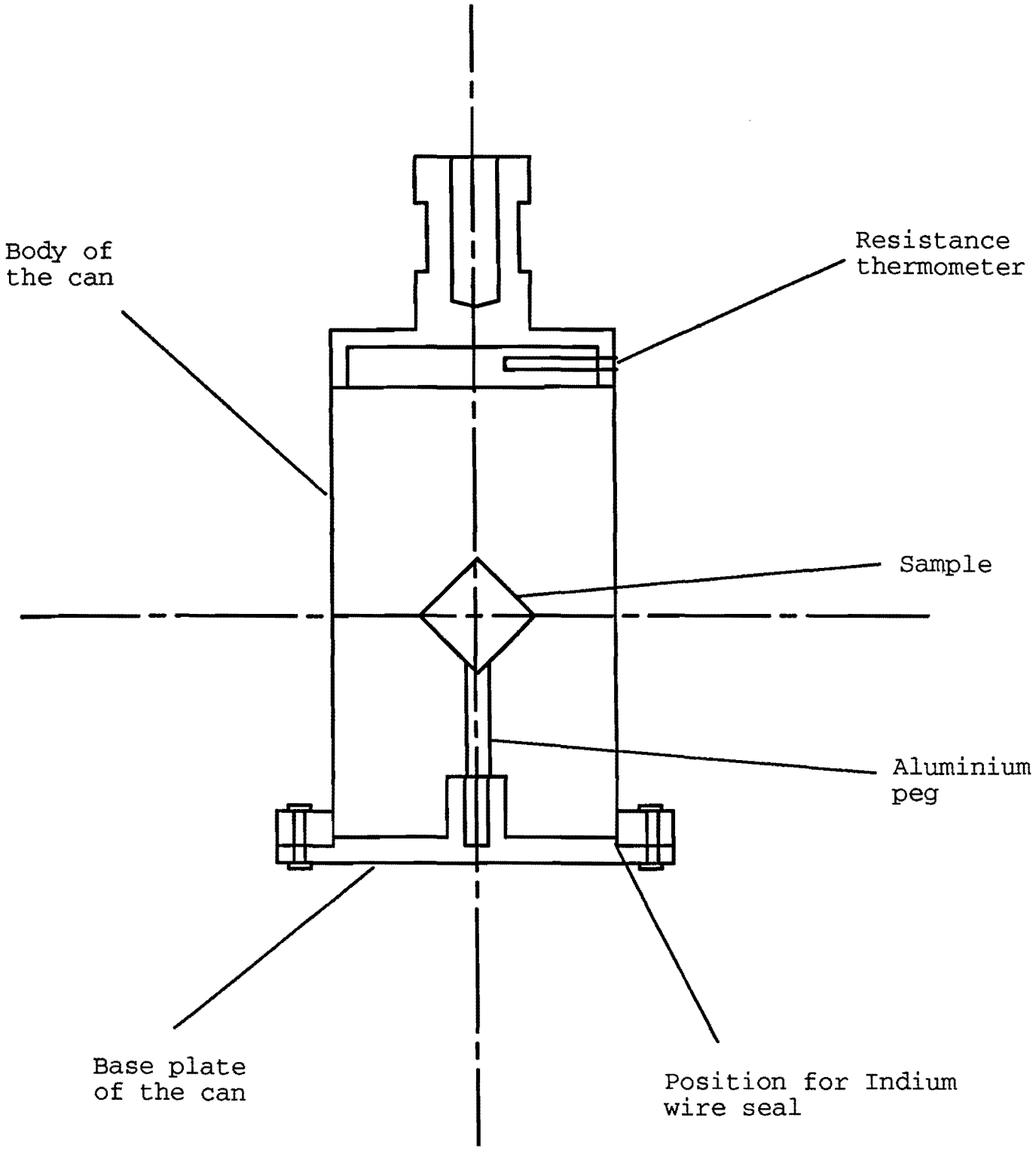

Figure 5: A sketch is shown of the aluminium can used to hold the sample during the critical scattering measurements.

8 (untapped) holes which allow the two halves to be bolted together. In the centre of the base is a location hole into which can be inserted an aluminium peg which holds the sample. The top of the body has an 8mm thread tapped into it to allow attachment to a closed cycle refidgerator.

Although we have always mounted our samples using an aluminium peg this is not the only method available. However the general precautions we outline in the following for masking the peg we have used for mounting apply equally well to any form of mount. The peg is usually preshaped to fit the contours of the pre-oriented sample which is attached by means of an adhesive such as Kwik-Fill or by placing a thin aluminium strap around the sample which can be bolted through the peg. The peg is then inserted into the base of the can and fixed in position by means of a small grub screw. Before the can is assembled the aluminium peg is masked off from the neutron beam using a combination of thin cadmium sheets and gadolinium foil to eliminate the aluminium powder lines that can result. If Gd foil is used it is normally held in place with thin wire. If glue or Kwik-Fill is used it is essential to cover it using Cd/Gd sheet/foil or gadolinium based paint. It needs to be remembered that critical scattering is considerably weaker than Bragg scattering and the incoherent scattering from hydrogen in glues must be avoided at all costs.

As noted earlier, to ensure that the sample will be in good thermal contact with its surroundings the sample can is filled with helium gas to act as a temperature exchange medium. This is achieved by assembling the sample can inside a glove bag containing a helium gas atmosphere. To seal the helium gas inside the can indium wire is used as a "gasket" between the base and the body. This wire flattens out as the bolts are tightened

to form the seal.

Finally, there is a resistance thermometer mounted in the body of the can which is used to measure the temperature of the exchange gas and hence indirectly the temperature of the sample.

3.3 Temperature Control, Monitoring and Analysis

The ISIS instruments all create/maintain .LOG files for the sample environment blocks during instrument runs. While a particular run is in progress this file is stored in the INST_DATA directory and is called INST.LOG. When a run has been completed this INST.LOG file is renamed to a filename of the form PRS10153.LOG, the 1st 3 letters are the instrument name and the 5 numbers are the relevant run number. In order for the sample temperature(s) to be stored in the .LOG file it is necessary to use a command of the form CSET TEMP/LOG (note the name TEMP can be replaced with either TEMP1 or LAKES on PRISMA). A detailed description of this command is given in section(2.11) of the PRISMA Operating Program Manual [7].

If the temperature values have been (are being) recorded in a .LOG file then they can be accessed with one of the GENIE macros TP, TPC or AT. These are described in detail in section(7) of the PRISMA GENIE Data Analysis Manual [7]. The TPC and TP commands allow GENIE to plot a graph of temperature against time during the run. TPC is used for the the current run and TP is used for a run that has already been completed. The AT command calculates the mean and standard deviation for the temperatures recorded in a .LOG file. The output from these commands can therefore be

used to assess and quantify the temperature stability during a run.

3.4 Resolution Considerations

The width in reciprocal space of the measured intensity in a critical scattering experiment comes from two sources, the width of the intrinsic critical scattering lineshape itself (which is $\sim 2\kappa$) and the resolution width of the neutron diffractometer. The resolution function for a time of flight diffractometer has been discussed in detail in appendix B of ref. [4] and we will not repeat it here. The relevant point is that in order to measure statistically accurate values for κ, the width of the resolution function (due to the diffractometer) must be comparable in size to the κ values. Since κ is strongly temperature dependent (cf. equation(3)), going to zero at T_c, this condition can't hold true at all temperatures. In effect the resolution width of the diffractometer dictates how close in reduced temperature t one can get to the transition temperature. Since the power law relations (equations (3), (4) and (5)) will only hold true for t small [1, 2] one certainly wishes to make accurate measurements of κ in this small t limit. Obviously it is difficult to give a precise indication of what constitutes t small and also good (narrow) resolution since these will depend upon experimental circumstances. However one would hope to get to $t \sim 0.001$ or better and to have the resolution width not much bigger than $\sim 5\times$ the smallest value of κ.

The major factors effecting the resolution width of the spectrometer are the energy of the incident neutrons E_i and the angular divergence of the Soller collimation. It is possible to calculate resolution widths (and to get contour maps of the resolution function) using

the PRSCAL program. Details on the various commands to do this are given in section 9 of the "The PRSCAL Manual" [7].

The trend of the resolution function is that for smaller values of E_i and the angular divergence of the collimation the narrower (better) the resolution width. However the choice of E_i is influenced by other criteria as well, notably E_i must be large enough to satisfy the quasi-static approximation (section(5.3)). As a consequence there will always have to be a compromise between resolution and the quasi-static approximation in the choice of E_i. A facet of the time of flight technique which can be useful in this case is that it is easy in the data analysis to merge data taken with different E_i values and consequently different wavevector regions of the critical scattering can be measured with different E_i values. In general one needs good wavevector resolution for small reduced wavevectors where the quasi-static approximation can be satisfied by smaller values of E_i and one doesn't need such good wavevector resolution at large reduced wavevectors where one needs larger E_i values to ensure that the quasi-static approximation is satisfied.

Although PRSCAL can calculate the resolution widths one should remember that this is only a calculation and one should certainly measure the resolution widths for the spectrometer during an experiment. This can be done by scanning one or (preferably) more Bragg peaks in the crystal at one (or more) value(s) of E_i. This should be done in the radial (time of flight), transverse (rocking curve) and out of plane (tilt) directions. These measured widths can then be compared with those predicted by PRSCAL and a complete set of resolution function parameters determined. We have usually found that we have been able to get good agreement between PRSCAL and experiment simply by

varying the value of the sample mosaic spread parameter. When measuring these Bragg peak widths to determine the resolution function it is important to avoid the effects of detector saturation and extinction (see sections (4.2) and (4.3)).

4 Bragg Peak Intensity Measurements

4.1 Introduction

If a Bragg peak in a crystal is specifically associated with the long range order corresponding to a particular phase then the intensity of that Bragg peak as a function of temperature is usually given by equation(5). This intensity against reduced temperature relation arises because the Bragg peak is proportional to the square of the order parameter. As an example, for an anti-ferromagnet the order parameter is the staggered magnetisation which is given by

$$M = M_0 t^{\beta} \tag{9}$$

and the Bragg peak intensity is given by $I \propto M^2$ [2, 3]. Therefore it is in principle possible to measure the critical exponent β simply by measuring the intensity of the Bragg peak as a function of temperature. In practice however there are difficulties with such a measurement that mean that β ends up being the least reliable of the critical exponents that can be measured with neutrons. We describe in the following sections what these problems/difficulties are and what (if anything) can be done about them. In the rest of this introduction however we'll briefly describe how the Bragg peak intensity can be measured.

The rocking curve width of a Bragg peak is usually too narrow for there to be any advantage in measuring it with a multi-detector arrangement. Instead we have used a single detector and performed a rocking curve of the Bragg peak. A specific scattering angle ϕ is chosen and the sample rotation angle is stepped through its Bragg peak value,

going far enough on either side to reach background. This scan is usually carried out by an SC command (see section(2.4) of the PRISMA Operating Program Manual [7]). At each step of the scan a radial time of flight spectrum is taken. This is repeated for a series of temperatures just below T_c and between each temperature a suitable equilibriation time is allowed.

The measured spectra in each rocking curve scan can be processed using the AA command (see section(4.4) of the PRISMA GENIE Data Analysis Manual [7]). A "narrow" time of flight window around the flight time corresponding to the Bragg peak is chosen and the time of flight spectra in each step integrated over this window. The output from AA is a rocking curve of integrated counts vs sample rotation angle. This curve can either be directly integrated or (better) fitted (see the FF function described in section(8.1) of ref. [7]) to obtain the total integrated intensity (integrated over both ToF and angle) for the Bragg peak.

These integrated intensities can then be fitted to equation(5) over a suitable range of reduced temperature to obtain the β exponent.

4.2 Detector Saturation

All neutron scattering detectors have a "dead time" effect, when a neutron is counted in the detector there is a period of time after the detector has "counted" during which it cannot count again. Consequently any neutrons arriving at the detector during this dead time will be "lost". For a He gas detector this time is $\sim 10 \rightarrow 30\mu$s, which is comparable the width of a Bragg peak measured in time of flight. At a spallation source the neutrons

are produced in pulses and their flight time is measured during a "frame" between two pulses. At ISIS the latter is 20 milliseconds long and there are 50 frames per second. Thus if the intensity measured in a particular Bragg peak exceeds an average rate of 1 count/frame (50 counts/second) then there is a danger that the measured count rate is not the "true" count rate and hence the nominal Bragg peak intensity will be incorrect. Note this does not mean that there must only be 1 count/frame (50 counts/second) in total in a frame, there can be many Bragg peak orders etc. in a 20ms frame. Instead it means that within the time window corresponding to the Bragg peak of interest the intensity should not exceed 1 count/frame. Since by definition this intensity goes to zero at T_c one can always simply raise the temperature to achieve this condition. Alternatively (a better solution is that) one can attenuate either the incident or scattered neutron beams to reduce the Bragg intensity to a suitable level.

4.3 The Effect of Primary Extinction

The effect of detector saturation could lead to the measured Bragg peak intensity being "incorrect" and primary extinction can cause a similar distortion. However whereas detector saturation can be easily remedied with an attenuator primary extinction cannot (if at all) be easily remedied. A full description of primary extinction is given in chapter(3) of Bacon [8]. In short, if the intrinsic scattering strength of a Bragg peak is large then it is possible for all the neutrons in the incident beam that can be scattered by the crystal to be scattered by only a fraction of the volume of the single crystal sample. As a consequence the measured intensity will not reflect the scattering from the full volume of the crystal.

This is a very serious effect for a measurement of β because the primary extinction is strongly temperature dependent. Close to T_c the order parameter/Bragg peak is weak and there is little (if any) extinction, but on cooling, as the order parameter/Bragg peak grows so will the effect of the extinction increase. Consequently the measured Bragg peak intensity will not directly reflect the square of the order parameter but will be attenuated by an unknown and temperature dependent factor due to the primary extinction.

There are various possibilities one can try to overcome or quantify the effect of primary extinction. The degree of extinction depends upon the strength of the Bragg peak and the energy of the incident neutrons. One can "reduce" the strength of the Bragg peak either by means of working with an intrinsically weaker Bragg peak or working closer to the transition temperature (where the order parameter is small). An analysis of the primary extinction factor shows (see Bacon chapter(3) [8]) that its degree varies with the inverse of the incident neutron energy. Thus one could work with high neutron energies to avoid primary extinction. However as will be seen in sections(5.5) and (4.4) there are reasons not to use high neutron energies. In practice one would be well advised to measure more than one Bragg peak and with different incident neutron energies in order to get a handle on how much primary extinction is effecting the measured β value.

There is a special case where one may "luckily" avoid primary extinction. If the material in question is absorbing then the penetration depth of the neutron beam into the crystal may be small enough that there is never any primary extinction effect. Of course, in an absorbing material one won't see much of a scattered intensity for the Bragg peak anyway so this isn't much of an advantage.

4.4 Contamination by Critical Scattering

At temperatures below T_c the scattering around a Bragg peak position comes from two components (cf. equation(13) in section(5.2))the Bragg peak and the critical scattering. At temperatures well below T_c the Bragg peak is very strong and the critical scattering weak so that the integrated intensity measured in a rocking curve is predominantly due to the Bragg peak. However close to T_c this is not necessarily so since the Bragg peak has become weak (it goes to zero at T_c) and the critical scattering is growing (its amplitude diverges at T_c). What one observes for the integrated intensity against temperature is an S-type curve, an example of which is shown in figure(6). Well below T_c the high intensity is due to the Bragg peak. This intensity falls with increasing temperature but does not go to zero at T_c but instead there is a tail due to the critical scattering extending above T_c. The problem is, for the data points just below T_c how much intensity is due to the Bragg scattering and how much is due to critical scattering. One cannot include data points close to T_c when fitting to equation(5) because of this problem. In effect there is a temperature range just below T_c which is "forbidden" in determining β from from Bragg peak intensity measurements.

The factor that governs the size of this forbidden temperature range and hence the extraction of the β exponent is the size of the resolution volume. This can be seen by considering how the measured intensity at the middle of the Bragg peak rocking curve is obtained. Since the Bragg peak is a sharp function (in principle a δ-function) it just projects out the height of the resolution function. However because the critical scattering

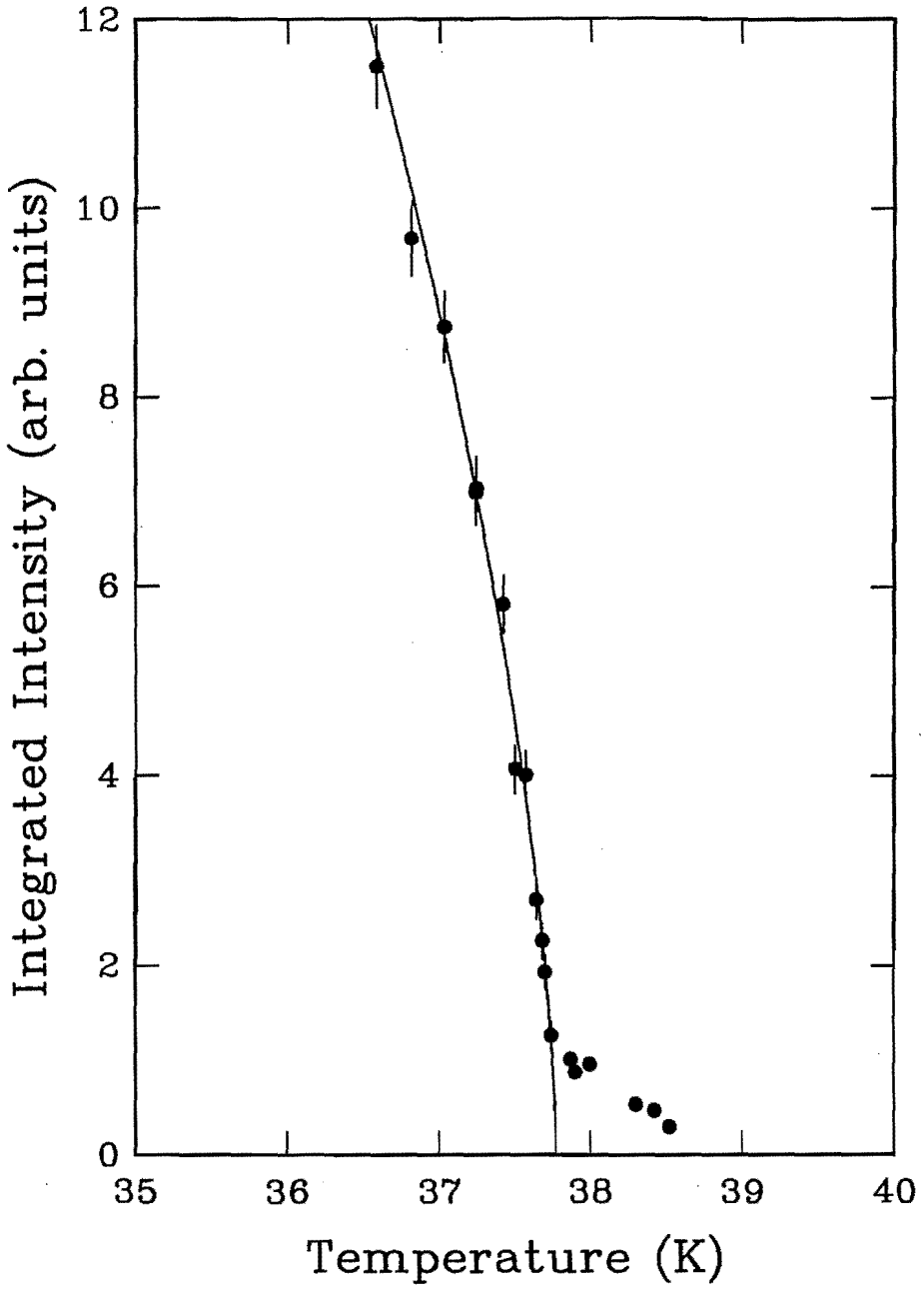

Figure 6: The integrated intensity at the (1,0,1) antiferromagnetic Bragg peak position in $FeCO_3$ is shown as a function of temperature. The solid line is the result of a fit to equation(5) for data well below the transition temperature.

is broad it is integrated over the volume of the resolution function. If we increase the resolution function volume we will increase the critical scattering contribution but not change the Bragg peak contribution. Thus the better (smaller) the resolution function volume the better is the rejection of the critical scattering contribution to the integrated intensity.

Therefore in order to reduce the contamination of the integrated intensity by critical scattering close to T_c one would like to work with small E_i values to reduce the resolution function volume.

4.5 Summary — The E_i Compromise

From the preceding sections it should be clear that there are contradicting requirements for the best value of E_i to measure the integrated Bragg intensity. To avoid primary extinction one would like E_i large while to avoid contamination of the Bragg intensity by the critical scattering then one would like E_i small. As noted earlier it is a good idea to perform measurements with more than one value of E_i in order to get a handle/self-consistency check on these problems. It is also hopefully clear why β is the least reliable exponent one can obtain by neutron scattering.

5 Critical Scattering Measurements

5.1 Introduction

In this section we deal with some of the points relating to the measurement of the critical scattering itself. One of the important conditions that must be satisfied when measuring the critical scattering is the quasi-static approximation. In sections(5.2) and (5.3) we describe how the correlation function for critical scattering is related to the partial differential cross-section for neutron scattering and the criteria a diffraction measurement needs to satisfy in order that the critical scattering can be accurately measured. For the purpose of description we will specifically consider a magnetic phase transition but the same arguments apply equally well to structural phase transitions. Following this theoretical background we discuss the practical aspects of measuring critical scattering. In section(5.4) we describe how multi-detector scans can be used to measure the critical scattering. A brief cautionary note about the rare (but possible) effect of multiple scattering in a critical scattering measurement is included in section(5.5). Finally section(5.6) discusses the analysis of the measured critical scattering spectra.

5.2 The Correlation Function

The magnetic critical scattering measured in a neutron scattering experiment is the Fourier transform of the spatial distribution of the magnetic moments (spins) in the sample. Just above T_c these spins have short range order and form fluctuating micro-regions. The size distribution of these regions can be described by a correlation function

which in its most general form measures the correlation between the fluctuations of the spin components away from their mean values. It can be written as [1]

$$\Gamma_{ij}^{\alpha\beta} = \langle (S_i^{\alpha} - \langle S_i^{\alpha} \rangle)(S_j^{\beta} - \langle S_j^{\beta} \rangle) \rangle \tag{10}$$

where α, β represent the real space spin components x, y, z of the ith and jth magnetic ions in the sample. This form of the correlation function is known as the *static* (or equal time) correlation function since it represents the spin correlation between sites i and j at the same instant in time. The Fourier transform of the correlation function given in equation(10) can be written as

$$\Gamma^{\alpha\beta}(\mathbf{Q}) = \sum_{ij} \exp[i(\mathbf{Q}.\mathbf{r}_{ij})]\ \Gamma_{ij}^{\alpha\beta} \tag{11}$$

This correlation function can be related to the partial differential cross section for magnetic neutron scattering which is given by [2]

$$\frac{d^2\sigma}{d\Omega dE_f} = \frac{1}{N}\left(\frac{k_f}{k_i}\right)\frac{(\gamma \mathbf{r}_0)^2}{2\pi\hbar}\sum_{\alpha\beta}(\delta_{\alpha\beta} - \hat{Q}_{\alpha}\hat{Q}_{\beta})g^2\mu_B^2|f(\mathbf{Q})|^2 \times \int \exp[-iEt/\hbar]\sum_{ij}\exp[i(\mathbf{Q}.\mathbf{r}_{ij})]\langle S_i^{\alpha}(0)S_j^{\beta}(t)\rangle\ dt \tag{12}$$

Integrating the partial differential magnetic cross section over all energy transfers $\Delta E = E_i - E_f$ with the important assumption that $\mathbf{Q}$ remains fixed leads to the result

$$\begin{aligned} \int \frac{d^2\sigma}{d\Omega dE_f}\, d\Delta E &= K_1(\delta_{\alpha\beta} - \hat{Q}_{\alpha}\hat{Q}_{\beta})\sum_{ij}\exp[i(\mathbf{Q}.\mathbf{r}_{ij})]\langle S_i^{\alpha}(0)S_j^{\beta}(0)\rangle \\ &= K_1\left[\delta(\mathbf{Q})\sum_{\alpha}(1 - (\hat{Q}_{\alpha})^2)\langle S^{\alpha}\rangle^2 + \sum_{\alpha\beta}(\delta_{\alpha\beta} - \hat{Q}_{\alpha}\hat{Q}_{\beta})\Gamma^{\alpha\beta}(\mathbf{Q})\right] \end{aligned} \tag{13}$$

where K_1 represents all of the various co-efficients in equation(12). The first term in the square brackets is the magnetic Bragg peak scattering, where $\delta(\mathbf{Q}) = \sum_{ij}\exp[i(\mathbf{Q}.\mathbf{r}_{ij})]$ is

zero unless $\mathbf{Q}$ is equal to a reciprocal lattice vector. The second term is the correlation function defined above and a standard "model form" for $\Gamma(\mathbf{Q})$ is the structure factor $S(\mathbf{q})$ given in equation(1) where $\mathbf{q} = \mathbf{Q} - \boldsymbol{\tau}$ and $\boldsymbol{\tau}$ is the ordering wavevector (Bragg peak position). Therefore if in a neutron scattering experiment it were possible to perform such an integration over energy at constant $\mathbf{Q}$ the measured intensity would (apart from resolution effects) be equal to the correlation function. However measuring the partial differential cross section at different $\mathbf{Q}$ values and integrating over ΔE at each $\mathbf{Q}$ value would be an extremely time consuming (impossible ?) thing to do. Instead critical scattering is usually measured by neutron diffraction techniques. As a consequence the integral in equation(13) is not performed exactly but only approximately. The condition under which this is a good approximation is discussed in the next section.

5.3 The Quasi-Static Approximation

A diffraction experiment measures all of the scattering processes, both elastic and inelastic, that take place within the sample and which satisfy the relevant diffraction conditions. A diffraction measurment is therefore equivalent to carrying out an integration of $d^2\sigma/d\Omega dE_f$, over the energy transfer ΔE. It is not however exactly the integral given in equation(13) because the wavevector transfer $\mathbf{Q}$ does not remain fixed in this process. If however the variation in the wavevector $\Delta\mathbf{Q} = \mathbf{Q} - \mathbf{Q}_0$ where $\mathbf{Q}_0$ is the nominal (elastic) wavevector is only small over the range of energy transfers (ΔE) involved then such a diffraction measurement will be a good approximation to equation(13). Experimental conditions that meet this requirement are said to satisfy the *quasi-static approxima-*

tion [2, 3].

The relationship between $\Delta\mathbf{Q}$ and ΔE for a two axis diffractometer at a reactor source has been considered before [2, 3, 6] and is given by [3]

$$\Delta\mathbf{Q} = \frac{\Delta E}{2E_i}\mathbf{k}_f \tag{14}$$

For the time of flight technique a similar result can be derived [5] and is

$$\Delta\mathbf{Q} = \frac{\Delta E}{2E_i}\left[\frac{(L_f/L_i)\mathbf{k}_i + \mathbf{k}_f}{1 + (L_f/L_i)}\right] \tag{15}$$

This is essentially the same result as equation(14) apart from the extra terms involving the ratio of the flight paths (L_i is the moderator to sample distance and L_f is the distance from the sample to the detector). However the exact value of the ratio L_f/L_i is not that important to the overall outcome.

The amount of variation in the wavevector $\Delta\mathbf{Q}$ involved in the diffraction measurement (at either a reactor or a pulsed source) can be estimated from equations(14) and (15) by setting $\Delta E \approx \Delta E_{cs}$, where ΔE_{cs} is the energy width of the critical scattering. Hence the condition for $\Delta\mathbf{Q}$ to be small is $E_i \gg \Delta E_{cs}$. Under these conditions the quasi-static approximation is said to be satisfied and the measured diffraction pattern can be considered equal (to a good approximation) to the correlation function of equation(13). Detailed analysis by Tucciarone *et al.* [6] using accepted models for the energy dependence of the critical fluctuations, suggests that a value of $E_i \geq 5\ \Delta E_{cs}$ [3] would be sufficient. Since ΔE_{cs} is usually unknown (it would be an unusual state of affairs if the wavevector width were unknown but the energy width were known) it is usually necessary to estimate the energy width. For Ising like (strong uniaxial anisotropy) systems the energy width is

usually quite narrow, of the order of tenths of an meV, while for more isotropic systems (X-Y, Heisenberg) it is more of the order of meV. Obviously the value will differ system to system and will be related to the transition temperature, the higher T_c the wider the energy width.

5.4 A Critical Scattering Scan

Above T_c the critical scattering can be measured using a multi-detector arrangement. As indicated in the earlier sections this usually involves measuring a fan of radial time of flight scans and interleaving or merging together these fans to make a grid of measured data covering the region in reciprocal space occupied by the critical scattering. In carrying out this interleaving/merging we have in our experiments left the scattering angles for the multi-detector fixed and varied the sample rotation angle. This is not the only possibility, one could leave the sample angle fixed and step the detector angle to achieve the same effect. There is an advantage to the former technique however because it requires fewer normalisation runs to be performed.

The data collected in these interleaving fans can be processed using the VCRS macro in GENIE and displayed using the PRSPLOT6 program. A detailed description of VCRS is given in section(6.2) of the PRISMA GENIE Data Analysis Manual [7]. An important point here is that in order to accurately process, display and subsequently fit the critical scattering data a vanadium calibration run is required. In the multi-detector configuration different detectors are being used to measure different paths through the critical scattering. These detectors will almost certainly have different efficiencies. Also because

they are at different scattering angles they will also have different resolution volumes. In order for displayed data to be visually consistent both of these effects must be compensated for. The vanadium calibration is simply a run at the same scattering angles for the detectors using a vanadium rod rather than the sample. Because vanadium is an incoherent scatterer normalising the measured critical scattering spectra with the vanadium spectra compensates for both detector efficiency and resolution volume. It should be noted that in the data analysis (described in the next section) the resolution volume effect is taken into account but the vanadium calibration is still needed to correct for the efficiency variation.

A vanadium calibration run is required for each of the angular settings at which the multi-detector is used. This is why it is easier to step the sample rather than the multi-detector. Since one would like during an experiment to look at the data as it is being taken it is a good idea to perform some vanadium calibration runs before starting the experiment proper. If you change your mind during the experiment and perform some runs at unexpected scattering angles then you should make sure that you have enough time at the end of the experiment to get the necessary calibration runs done. We have found that this vanadium calibration approach has made it quite straightforward for us to combine in the fitting procedure (section(5.6)) data taken at different ranges of scattering angle settings for the multi-detector without too much difficulty.

The output file from the VCRS macro can be read directly into the PRSPLOT6 program, which allows the data to be displayed. This can be either as a contour map or as a relief map, an example of which is shown in figure(7). There are various commands

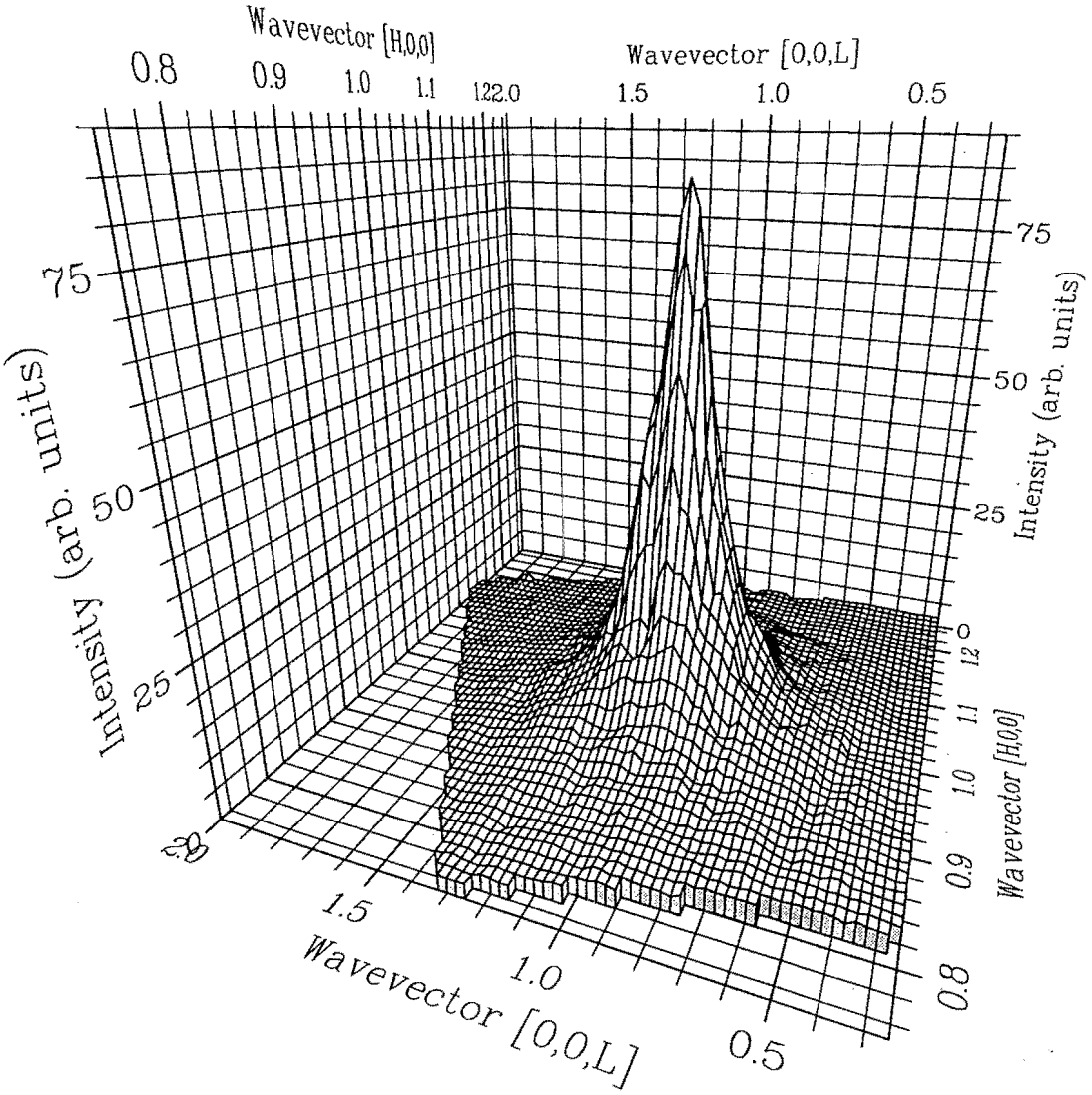

Figure 7: A relief map plot of the critical scattering measured from $FeCO_3$ at a temperature of 38.10 K is shown

in PRSPLOT6 (see the manual [7]) which allow the way in which the data is displayed to be varied. There is also a command X/P which allows cuts through the grid of data to be made so that the data can be examined along specific directions. An example of such a cut is shown in figure(8).

5.5 Multiple Scattering

Above T_c the critical scattering occurs around the ordering wavevector, ie. the Bragg peak position in reciprocal space. However above T_c there should be no Bragg scattering because there is no long range order. In certain (rare) circumstances it is however possible to observe a "false" Bragg peak at the ordering wavevector due to multiple scattering from Bragg peaks in the sample. We have observed this in an experiment on $FeCO_3$ [5] and it has been a problem in measurements on MnF_2 [3]. What happens in these circumstances is that the incident neutron beam is initially scattered by a Bragg peak with wavevector $\boldsymbol{\tau}_1$ (which is not equal to the critical scattering Bragg peak ordering wavevector $\boldsymbol{\tau}_0$). However before these scattered neutrons can exit the sample they are scattered a second time by another Bragg peak with wavevector $\boldsymbol{\tau}_2$. If $\boldsymbol{\tau}_0 = \boldsymbol{\tau}_1 + \boldsymbol{\tau}_2$ then these doubly scattered neutrons will be scattered into the detector as if they had been singly scattered by $\boldsymbol{\tau}_0$ and hence they appear to be a Bragg peak at $\boldsymbol{\tau}_0$. It should be noted that these doubly scattered neutrons must have the same wavelength as if they had been singly scattered. The size of the sample is irrelevantly small compared to the length of the moderator to sample to detector flight path and therefore to be identified as having a wavevector of magnitude $|\boldsymbol{\tau}_0|$ the doubly scattered neutrons must have the same flight time (ie. wavelength) as

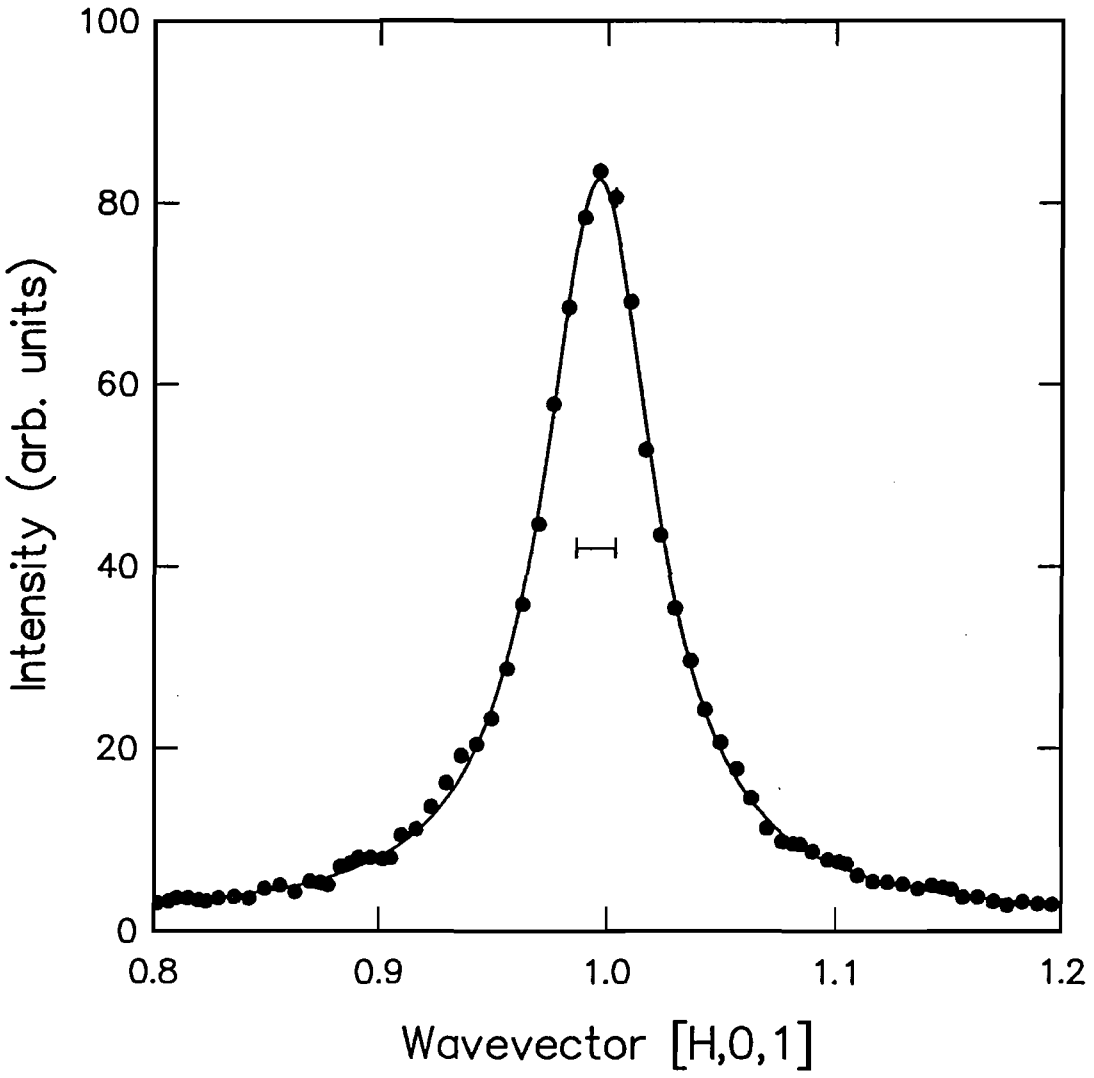

Figure 8: A cut along the (H,0,1) direction through the critical scattering from $FeCO_3$ at 38.10 K is shown

would the equivalent singly scattered neutrons.

As emphasised above this multiple scattering problem is a rare occurence and requires a conspiracy of co-incidences for more than one Bragg scattering process to be possible. Such co-incidence is much more likely if the incident neutron energy E_i is large. A simple way to test for multiple scattering and to find a wavelength/energy at which it is avoided is to perform a $\delta\phi = 2\delta\omega$ scan (as described in section(2.2.1)) corresponding to a radial scan through the false Bragg peak. The multiple scattering condition will only occur for a certain small wavelength/energy range and this should be apparent in the scan allowing for a choice of scattering conditions which avoid it.

5.6 Analysis of the Critical Scattering Data

As noted earlier in section(1.2) the measured intensity in the critical scattering is the convolution of the critical scattering lineshape (eg. equation(1)) and the resolution function for the time of flight neutron diffractometer. What one would like to extract from the critical scattering data set are the values of the κ's and χ's etc. which characterise the critical scattering at that particular temperature. In order to do this one must fit the experimental data to a model lineshape which has been convoluted with the resolution function. This is essentially the same situation as for critical scattering experiments carried out at reactor neutron sources the only difference is the number of data points. At a reactor source one would collect $\sim$ 100 data points while in our time of flight experiments we collect $\sim$ 3000 to 15000 data points. The fitting of such a large amount of data is a major task and in the following we'll describe how we have approached this.

Obviously this involves a computer program to actually carry out the fitting and the program we have written is called CRTFIT. In appendix A we describe the input and output files for this program.

The fitting program minimises the least squares *agreement factor* given by

$$A = \sqrt{\frac{1}{N-K}\sum_{i=1}^{N}\left(\frac{I_i^{obs} - I_i^{cal}}{\sigma_i}\right)^2} \tag{16}$$

where N is the number of data points, K is the number of adjustable parameters, I_i^{obs} and I_i^{cal} are the experimentally observed and theoretically calculated intensities and σ_i the experimentally observed (standard deviation) error, for the i^{th} data point. This is done by an iterative non-linear least squares method utilising a Marquardt algorithm [9] to find the values of the adjustable parameters which produce the set of calculated values I_i^{cal} which give the minimum value of A. It can be shown that A has an expectation value in the statistical sense of 1 for uncorrelated errors drawn from a normal distribution. Thus a good fit to the data would be expected to have a value for A of around 1. However there is more to a good fit that just a good agreement factor, a good fit should not have any systematic (correlated) differences between the experimental and theoretical values. It is necessary to check for such a systematic discrepancy "visually". One way of doing this is to take cuts through the observed and calculated map files and compare them. This can be "automated" using the ZXMAP [10] program which will produce an output file containing all of the spectra from an experimental and the equivalent calculated map files ready for plotting. Another approach is to make a grid plot of the residuals. The residual

for the i^{th} data point is given by

$$r_i = \frac{I_i^{obs} - I_i^{cal}}{\sigma_i} \tag{17}$$

ie. it is the normalised difference between the observed and calculated values. In the CALULATED.MAP file produced by CRTFIT (see appendix A) the final column of the output (which would be the error column in an experimental data file) contains the value of the residual. It is possible to display a colour grid map of the residuals in PRSPLOT6 by loading the CALCULATED.MAP file and using the command D/I/E W1 (with the appropriate level values set, remember r_i can be both $+ve$ and $-ve$). If there are no systematic correlations this plot should look like a random mess of colours. Correlations should show up as regions of a particular colour in the plot.

At each iteration in the Marquardt algorithm a value must be calculated for each of the data points using the theoretical values for κ etc. It is this calculation for the 1000's of data points that consumes all of the time in the computer program. The convolution integral involved in this calculation can be written as ;

$$I(\mathbf{Q}_0) = \int R(\mathbf{Q}_0 + \Delta\mathbf{Q}) S(\mathbf{Q}_0 + \Delta\mathbf{Q} - \boldsymbol{\tau}\ ) d\Delta\mathbf{Q} \tag{18}$$

where $S(\mathbf{q} = \mathbf{Q}_0 + \Delta\mathbf{Q} - \boldsymbol{\tau}\ )$ was given in equation(1) and $R(\mathbf{Q}_0 + \Delta\mathbf{Q})$ is the resolution function which is given by ;

$$R(\mathbf{Q}_0 + \Delta\mathbf{Q}) = \left(\frac{1}{V}\right) \exp\left[-\frac{1}{2}\left(\left(\frac{\Delta Q_T}{\sigma_{DT}}\right)^2 + \left(\frac{\Delta Q_V}{\sigma_{DV}}\right)^2\right)\right] \times \exp\left[-\frac{T^*}{\tau}\right] \operatorname{erfc}\left[\frac{1}{\sqrt{2}}\left(\frac{\sigma_0}{\tau} - \frac{T^*}{\sigma_0}\right)\right] \tag{19}$$

where

$$\sigma_{DV} = \sqrt{(\sigma_{SV}Q_0)^2 + (k_0)^2(\sigma_{1V}^2 + \sigma_{EV}^2)} \quad (20)$$

$$\frac{1}{\sigma_{EV}^2} = \frac{1}{\sigma_{2V}^2} + \frac{1}{\sigma_{3V}^2} \quad (21)$$

$$\sigma_{DT} = \frac{1}{2}Q_0\sqrt{\sigma_{1H}^2 + \sigma_{EH}^2 + 4\sigma_{SH}^2} \quad (22)$$

$$\frac{1}{\sigma_{EH}^2} = \frac{1}{\sigma_{2H}^2} + \frac{1}{\sigma_{3H}^2} \quad (23)$$

$$\sigma_0 = \chi_0 \cot\left(\frac{|\phi|}{2}\right)\sqrt{\frac{\sigma_{1H}^2\sigma_{EH}^2 + \sigma_{1H}^2\sigma_{SH}^2 + \sigma_{EH}^2\sigma_{SH}^2}{\sigma_{1H}^2 + \sigma_{EH}^2 + 4\sigma_{SH}^2}} \quad (24)$$

$$T^* = \left(\frac{\chi_0}{Q_0}\right)\left[\Delta Q_L + \frac{\sigma_{1H}^2 - \sigma_{EH}^2}{\sigma_{1H}^2 + \sigma_{EH}^2 + 4\sigma_{SH}^2}\cot\left(\frac{\phi}{2}\right)\Delta Q_T\right] \quad (25)$$

$$\chi_0 = m_N\left(L_i + L_f\right)/\hbar k_0 \quad (26)$$

$$V = \left(\frac{1}{\chi_0}\right)\sigma_{DV}\sigma_{DT}\tau Q_0 \exp\left[-\frac{1}{2}\left(\frac{\sigma_0}{\tau}\right)^2\right] \quad (27)$$

which is essentially equation B.6 from ref. [4] (we have used identical notation to that paper) except that it has been normalised by the resolution volume V to account for the vanadium normalisation of the data.

The convolution integral, equation(18), is three-dimensional and one of the dimensions, the integral over the out of plane terms in ΔQ_V, can be done analytically. This leaves the in-plane components in ΔQ_L and ΔQ_T to be done numerically. In order to do this one must first determine the limits for the numerical integrals. This can be done by numerically calculating the 1% contour level of the in-plane component of the resolution function (in CRTFIT this is done by the same algorithm as used in PRSCAL to plot the resolution function contours) and then calculating the rectangle of minimum area which encloses this contour. In order to numerically evaluate the integral within this volume

an adaptive Monte-Carlo method can be employed. In this method the rectangle is further divided into smaller rectangles. A pass is carried out through each of these smaller rectangles in which in each small rectangle a fixed number (eg. 20) of randomly chosen points are evaluated. After the passing through the small rectangles the overall estimate of the calculated intensity (convolution integral plus background) is calculated along with its accuracy. Also the relative contribution of the smaller rectangles to the total and the error in the total is calculated. If this contribution is such that it will not influence the accuracy of the total integral when compared to the preset accuracy for the calculation then the relevant small rectangle is dropped from the calculation. Successive passes are made through the small rectangles until the overall intensity value is accurate to less than a preset accuracy. In our case we have usually used a 1% accuracy. This method has the positive feature that it only takes a few passes to accurately calculate the value of the intensity in regions where the convolution integral is small (eg. background regions) but will make sure that in regions where the convolution integral may be large and/or the integrand rapidly varying that enough sampling points are used to get an accurate value. In short, it "transfers" processing effort from regions of the data set where the calculated values are easy to evaluate to those regions where they are difficult to evaluate.

6 Summary

Neutron diffraction is a powerful technique for studying critical phenomena and the time of flight method provides a means of rapidly mapping out the critical scattering. In this guide we have tried to point out some of the practical things that need to be thought about for doing/analysing such an experiment. As a consequence we have necessarily had to belabour the problems/difficulties that can arise. This doesn't mean they will happen during an experiment but since "forewarned is forearmed" we hope that the guide will help people to avoid them or at least to recognise them.

In a series of brief one line summations the following points are worth remembering in order to do a good time of flight critical scattering experiment ;

- good temperature control and stability is essential
- the sample mount should be well shielded
- the quasi-static approximation must be satisfied (E_i should be large enough)
- the wavevector resolution should be good enough to measure κ close to T_c (to $t \sim 0.001$ or better)
- vanadium runs need to be done for normalisation if a multi-detector configuration is used
- measurements of Bragg peak widths should be made to determine the parameters for the resolution function

- check for and avoid detector saturation in Bragg peak measurements
- checks for the effect of primary extinction on the Bragg peak intensities should be made

Acknowledgements

We gratefully acknowledge the financial support of a research grant (GR/K-04989) from the United Kingdom Engineering and Physical Sciences Research Council (EPSRC) for the support of this work. One of us (SJP) acknowledges the support of a CASE research studentship from the EPSRC and the ISIS Facility, RAL.

7 Appendix — The CRTFIT Program

7.1 Introduction

In this appendix we describe the CRTFIT program which can be used to fit time of flight critical scattering data. The contents of the appendix are correct at the time of writing but the reader should be aware that the program may vary in the future depending upon circumstances. There are versions of the code available at RAL which will run on the VAX and ALPHA computers and also a version which runs on SUN computers. The source code is written in Fortran 77 and should be portable to most machines with an appropriate compiler because there are no proprietry software libraries used. In order to run the programs on the ISIS computers you can use the command lines

```
$ RUN PRISMA_KNH_CRIT:CRTFIT          (on the Vax machines)

$ RUN PRISMA_KNH_CRIT_ALP:CRTFIT      (on the Alpha machines)
```

if you have executed the PRISMA_GENIE_SETUP command file. It should be noted that these programs will take a considerable amount of time to run and must be run in batch mode rather than interactively.

The necessary input files for the program are, the data file, a resolution parameters file and a fitting parameters file called FITPMS.DAT. The data file should be in the format of the CRITICAL.OUT file produced by the VCRS macro [7]. It should contain

all of the spectra (from runs with different E_i if necessary) that are to be fitted. The format of the FITPMS.DAT and resolution parameters file are discussed in sections(7.2) and (7.3). The output files from the program are a calculated values file called CALCULATED.MAP, a results file containing the parameter values at each iteration of the fitting and a final parameters file called FITPMS.NEW which is in the same format as the FITPMS.DAT file. The CALCULATED.MAP file is identical in structure to the input data file CRITICAL.OUT (same H,K,L values etc.) except that the data values are replaced by the calculated values and the data errors replaced by the residuals, ie. the difference between data and calculated values divided by the data error value. The PRSPLOT6 program can be used to plot contour/relief maps or extract cuts through the CALCULATED.MAP file.

The CRTFIT program will fit a selection of peak types to the data. In section(7.2) we will describe how these peaks are selected, however in order to do this we must first define what the peak functions used are. There are 3 types of function available, a Lorentzian, a Lorentzian squared and a Gaussian.

The Lorentzian

$$L(A,\kappa_x,\kappa_y,q_x^0,q_y^0,\tau_x,\tau_y) = \frac{A}{1+\left(\frac{q_x-q_x^0-\tau_x}{\kappa_x}\right)^2\left(\frac{q_y-q_y^0-\tau_y}{\kappa_y}\right)^2+\left(\frac{q_v}{\kappa_v}\right)^2} \qquad (A.1)$$

The Lorentzian Squared

$$L2(B,\kappa_x,\kappa_y,q_x^0,q_y^0,\tau_x,\tau_y)=\frac{B}{\left[1+\left(\frac{q_x-q_x^0-\tau_x}{\kappa_x}\right)^2\left(\frac{q_y-q_y^0-\tau_y}{\kappa_y}\right)^2+\left(\frac{q_v}{\kappa_v}\right)^2\right]^2} \quad \text{(A.2)}$$

In these two functions κ_x and κ_y are the two in-plane inverse correlation lengths and κ_v is the out-of-plane inverse correlation length. It should be noted that κ_v must be set equal to either κ_x or κ_y and the choice of which is made by setting a flag in the FITPMS.DAT file. The amplitude of the Lorentzian is A and of the Lorentzian squared is B, which because of the form in which the two functions are written means that these parameters are proportional to the relevant isothermal staggered susceptibility. The terms q_x^0, q_y^0 and τ_x, τ_y are "origins" for the critical scattering. The need for two sets of parameters defining the origin will become apparent in the discussion in section(7.2).

The Gaussian Function

$$G(C,q_x^0,q_y^0,\tau_{gx},\tau_{gy},\sigma_R,\sigma_T)=C\exp\left(-\frac{1}{2}\left[\left(\frac{\Delta q_R}{\sigma_R}\right)^2+\left(\frac{\Delta q_T}{\sigma_T}\right)^2\right]\right) \quad \text{(A.3)}$$

where

$$\begin{bmatrix}\Delta q_R\\ \Delta q_T\end{bmatrix}=\begin{bmatrix}\cos\theta & \sin\theta\\ -\sin\theta & \cos\theta\end{bmatrix}\begin{bmatrix}x^* & 0\\ 0 & y^*\end{bmatrix}\begin{bmatrix}q_x-q_x^0-\tau_{gx}\\ q_y-q_y^0-\tau_{gy}\end{bmatrix} \quad \text{(A.4)}$$

and θ is the angle between the radial direction through the point $(q_x^0+\tau_{gx}, q_y^0+\tau_{gy})$ and the x-axis. The "origin" $(q_x^0+\tau_{gx}, q_y^0+\tau_{gy})$ defines the centre of the Gaussian in reciprocal lattice co-ordinates, however the principle axes of the Gaussian are assumed to be along the radial and transverse directions with respect to the radial direction through

the point $(q_x^0 + \tau_{gx}, q_y^0 + \tau_{gy})$. Along these directions the Gaussian has standard deviations (= FWHM/2.35) of σ_R and σ_T respectively. These standard deviations are in units of Å^{-1} and hence the scaling by x^* and y^* as well as the rotation by θ for the co-ordinates $(q_x - q_x^0 - \tau_{gx}, q_y - q_y^0 - \tau_{gy})$. Unlike the Lorentzian and Lorentzian squared the Gaussian function is not convoluted with the resolution function.

7.2 The FITPMS.DAT File

The input file FITPMS.DAT provides the information on how CRTFIT should fit the experimental data. The structure of the file is perhaps most easily explained using an example. The following FITPMS.DAT file was used in fitting some of the Terbium critical scattering data ;

```
Trial fit of Terbium data with CRTFIT          TITLE
5 3 0 -1                                       NI,NPKS,IXY,IMSK
Flat-Backg  0.0000  0.0000  5.0000             B0
Back-slopx  0.0000 -1000.   1000.0             BQX
Back-slopy  0.0000 -1000.   1000.0             BQY
Centre-qx0  2.0050  1.9000  2.1000             QX0
Centre-qy0  0.0007  -0.100  0.1000             QY0
2                                              PEAK TYPE 2=LRZ+LRZ
Lor-amp-T+  2161.0  0.0001  90000.             A-PLUS
Lor-amp-T-  2606.0  0.0001  90000.             A-MINUS
Kappa-L(X)  0.0017  0.0005  0.5000             KAPPA-X
Kappa-T(Y)  0.0004  0.0002  0.5000             KAPPA-Y
Tau-x       0.1120  -1.000  1.0000             TAUX
Tau-y       0.0000  -1.000  1.0000             TAUY
3                                              PEAK TYPE 3=Gauss
Gauss-amp-  40.000  0.0001  90000.             C
Long-fwhm-  0.0330  0.0001  0.1000             FWHM-RADIAL
Tran-fwhm-  0.0145  0.0010  0.5000             FWHM-TRANSVERSE
Tau-g-x -   -0.112  -0.150  -0.050             TAUGX
Tau-g-y -   0.0000  -1.000  1.0000             TAUGY
3                                              PEAK TYPE 3=Gauss
Gauss-amp+  40.000  0.0001  90000.             C
```

```
Long-fwhm+  0.0330  0.0001  0.1000          FWHM-RADIAL
Tran-fwhm+  0.0145  0.0010  0.5000          FWHM-TRANSVERSE
Tau-g-x +   0.1120  0.0500  0.1500          TAUGX
Tau-g-y +   0.0000 -1.000   1.0000          TAUGY
15                                          NV
4 5 6 7 8 9 10 12 13 14 15 17 18 19 20      (INV(I),I=1,NV)
RESFIL.DAT                                  RES FILE NAME
OUTPUT.DAT                                  OUTPUT FILE NAME
TB754L.DIF                                  DATA FILE NAME
9 3                                         NL NT
```

The first line of the file is a title line which can be up to 72 characters long. The second line contains 4 integer control numbers. NI is the number of fitting iterations the program will perform. Next is NPKS the number of peak sets to be used in the fitting, which in the example is 3, one peak set consisting of two coupled Lorentzians and two Gaussian peaks. The different peak sets that are available are discussed later on. The 3rd parameter on this line is IXY, which chooses whether $\kappa_v = \kappa_x$ (IXY = 0) or $\kappa_v = \kappa_y$ (IXY = 1). The final parameter is IMSK, which deals with whether "masked" regions of data are fitted/calculated or not. Using another program, ZXMAP [10], it is possible to mask out regions within the grid of data in a CRITICAL.OUT type file so that they can be excluded from the fitting. If IMSK = 0 then no data points are excluded from the fitting. If IMSK = 1 then the masked data points are excluded from the fitting process but that the CALCULATED.MAP file will contain calculated values for the masked data points. Finally if IMSK = -1 then the masked points are both excluded from the fitting and are not calculated.

The next five lines in the FITPMS.DAT file are the parameters describing the background and overall origin for the data grid. All of the lines describing fitting parameters

have the same format given by

parameter name (10 characters)	initial guess value	minimum limit value	maximum limit value

The first 10 characters (including blanks) on the line are used as a name for the parameter. This is followed by 3 numbers, the first of which is the initial guess (or starting value) for that parameter in the iteration process. The other two values are minimum and maximum limits for the parameter, which will not be allowed in the fitting process to take values outside of these limits. The background function itself is given by ;

$$\text{Background} = b_0 + b_x(q_x - q_x^0) + b_y(q_y - q_y^0) \qquad \text{(A.5)}$$

where b_0 is the flat background and b_x, b_y are the slopes in the X and Y directions. The parameters q_x^0 and q_y^0 are the "overall" origin and are included in all of the peak functions (cf. equations (A.1), (A.2) and (A.3)).

The remaining fitting parameters are in blocks of parameters related to the peak sets. The first line of these blocks is an integer label value specifying the type of peak set, which are as follows ;

Peak set 1 : Lorentzian plus Lorentzian Squared

$$\text{Peak} = L(A, \kappa_x, \kappa_y, q_x^0, q_y^0, \tau_x, \tau_y) + L2(B, \kappa_x, \kappa_y, q_x^0, q_y^0, \tau_x, \tau_y)$$

The Lorentzian and Lorentzian squared share the same $\kappa_x, \kappa_y, \tau_x$ and τ_y values along with the overall origin values q_x^0 and q_y^0 shared by all functions. The origin values τ_x and τ_y allow this peak set to be shifted away from the overall origin. In the order they should appear in the FITPMS.DAT file the parameters for this peak set are $A, B, \kappa_x, \kappa_y, \tau_x$ and

τ_y. This peak set can be turned into a single Lorentzian or a single Lorentzian squared peak by setting $B = 0$ or $A = 0$ respectively.

Peak Set 2 : Two Coupled Lorentzians

$$\text{Peak} = L(A_+, \kappa_x, \kappa_y, q_x^0, q_y^0, +\tau_x, +\tau_y) + L(A_-, \kappa_x, \kappa_y, q_x^0, q_y^0, -\tau_x, -\tau_y)$$

This peak consists of two Lorentzians sharing the same κ_x and κ_y values, one at $+(\tau_x, \tau_y)$ and the other $-(\tau_x, \tau_y)$ away from the overall origin. The two Lorentzians have independent amplitudes A_+ and A_-. This peak set is particularly appropriate for situations where the critical scattering occurs as satellites around an overall origin (eg. as in Terbium). In the order that they should appear in the FITPMS.DAT file the parameters are $A_+, A_-, \kappa_x, \kappa_y, \tau_x, \tau_y$.

Peak Set 3 : Gaussian Function

This peak set is just the function defined in equation(A.3). The parameters τ_{gy} and τ_{gy} allow it to be shifted away from the overall origin. In the order that they should appear in the FITPMS.DAT file the parameters are $C, f_R, f_T, \tau_{gx}, \tau_{gy}$. The parameters f_R and f_T are the FWHM values in Å^{-1} for the radial and transverse widths of the Gaussian and are related to the σ_R and σ_T used in equation(A.3) by $f_R = 2.35\sigma_R$ and $f_T = 2.35\sigma_T$.

Internally within CRTFIT the parameters for the background, overall origin and peak sets are numbered 1, 2, 3,..., IK where IK is the total number of parameters. Both IK and the internal number of a parameter can be found by "counting down" the list of parameters in the FITPMS.DAT file. Of course it is not necessary (or even probably desirable) to vary all of the parameters when fitting. Therefore the line following the

blocks of peak set parameters contains the integer value NV, which is the total number of parameters which should be varied during the fitting process. The next line after this is the list of the internal numbers (NV of them) which define which parameters that are to be varied in the fit.

The next 3 lines are file names, all of which must be 10 or less characters. First is the name of the file containing the resolution function parameter values (cf. section(7.3)). Second is the filename where the results for each iteration in the fit should be written. Finally the third filename is the name of the CRITICAL.OUT format file containing the data to be fitted.

The final line of the FITPMS.DAT file relates to the adaptive Monte-Carlo integration. As described in section(5.6) the in-plane resolution function is enclosed by a rectangle which is subdivided into smaller rectangles. The integer values NL and NT define these smaller rectangles. The principle axes of the overall rectangle are usually close to being along the radial and transverse directions. Therefore the overall rectangle is divided into NL steps along its pseudo-radial and NT along its pseudo-transverse directions.

7.3 The Resolution Parameters File

In order to define the resolution function in the CRTFIT program a file of parameters is required. The name of this file is one of the parameters in the FITPMS.DAT file and its structure is given by ;

f_{1H}	f_{2H}	f_{3H}
f_{1V}	f_{2V}	f_{3V}
η_s		
τ_0	E_c	Γ
L		
x^*	y^*	
IQX	IQY	

The first two lines are the FWHM values of the divergences of the Soller collimation in degrees. These are converted into the standard deviations used in equations(19) to (27) in CRTFIT. The f_{1H} and f_{1V} are the horizontal vertical divergences between moderator and sample. The f_{2H} and f_{3H} values refer to the horizontal divergence after the sample and before the detector. The values of these two parameters depends on how the sample to detector collimation is physically determined. If there are two collimators back to back then f_{2H} and f_{3H} should represent one each. If alternatively there is only one collimator then f_{2H} should be set to its value and f_{3H} set to " $\sim \infty$ " (ie. a large number). Similar arguments apply to the vertical collimation between sample and detector (ie. f_{2V} and f_{3V}).

The η_s parameter is the FWHM in degrees of the sample mosaic spread. The parameters τ_0, E_c and Γ define the slowing down time of the neutron pulse as a function of energy as given by equation(17) of ref [4]. For the methane moderator the values $\tau_0 = 37.15\mu$s, $E_c = 9.0$meV and $\Gamma = 39.16$meV are appropriate. The parameter L is the total distance

from moderator to detector via the sample.

The remaining parameters x^*, y^*, IQX and IQY relate the X and Y directions used in the critical scattering functions and the H,K,L co-ordinates of reciprocal space. In CRTFIT the X and Y directions are assumed to be perpendicular. The integer values IQX and IQY indicate which of the H,K,L (values of 1,2,3 respectively) are to be used as X and Y co-ordinates respectively. Note the X and Y directions do not have to be only the (H,0,0), (0,K,0) or (0,0,L) directions, it could be for example that $IQX = 3$ and $IQY = 1$ for the X = $(0, 0, \mathrm{L})$ and Y = $(\mathrm{H}, \mathrm{H}, 0)$ directions respectively. The x^* and y^* values are the lengths in $\mathrm{\AA}^{-1}$ of the X and Y vectors. For example in a cubic crystal then Y = $(\mathrm{H}, \mathrm{H}, 0)$ would mean $y^* = \sqrt{2}\,(2\pi/a)$, while in a hexagonal crystal it would be $y^* = 4\pi/a$.

References

[1] J.M. Yeomans, "Statistical Mechanics of Phase Transitions", Oxford Science Publications, 1992

[2] M.F. Collins, "Magnetic Critical Scattering", Oxford University Press, 1989

[3] R.A. Cowley, Methods of Experimental Physics, Vol 23 Part C - Neutron Scattering, 18, Academic Press Inc, 1987

[4] M. Hagen and U. Steigenberger, New Considerations on a Multi-analyser Spectrometer Resolution Function, Nucl. Instr. and Methods in Phys. Res. B, 1992, 72, 239

[5] S.J. Payne, M.Phil Thesis, Keele University 1994

[6] A. Tucciarone et al., Quantitive Analysis of Inelastic Scattering in Two-Crystal and Three-Crystal Neutron Spectrometry; Critical Scattering from $RbMnF_3$, Phys. Rev. B, 1971, 4, 3206

[7] M. Hagen, Rutherford Appleton Laboratory reports, 1994

"The PRSCAL Manual", RAL-94-084

"The PRISMA Operating Manual", RAL-94-085

"The PRISMA GENIE Data Analysis Manual", RAL-94-086

"The PRSPLOT6 Manual", RAL-94-087

[8] G.E. Bacon, "Neutron Diffraction", 2nd Edition, Clarendon Press, Oxford, 1962

[9] P.R. Bevington and D.K. Robinson, "Data Reduction and Error Analysis for the Physical Sciences", 2nd Edition, McGraw-Hill, New York 1992

[10] S.J. Payne and M. Hagen, "The ZXMAP Program", (unpublished)